Met-myoglobin Association in Dilute Solution during Pressure-Induced Denaturation: an Analysis at pH 4.5 by High-Pressure Small-Angle X-ray Scattering

F. Spinozzi,*,† P. Mariani,† L. Saturni,† F. Carsughi,†,‡ S. Bernstorff,§ S. Cinelli,|| and G. Onori||

Dipartimento di Scienze applicate ai Sistemi Complessi, Università Politecnica delle Marche, Via Brecce Bianche, I-60131 Ancona, Italy, Institut für Festkörperforschung, Forschungszentrum Jülich, Germany, Sincrotrone Trieste, Strada Statale 14-Km. 163.5, in Area Science Park, 34012 Basovizza, Trieste, Italy, and Dipartimento di Fisica, Università di Perugia, CEMIN (Centro di Eccellenza Materiali Innovativi Nanostrutturati) and INFM-CRS SOFT, Via Pascoli, 06123 Perugia, Italy

Received: June 2, 2006; In Final Form: November 28, 2006

In this paper, we report on the original global fit procedure of synchrotron small-angle X-ray scattering (SAXS) data applied to a model protein, met-myoglobin, in dilute solution during temperature- and pressure-induced denaturation processes at pH 4.5. Starting from the thermodynamic description of the protein unfolding pathway developed by Hawley (Hawley, S. A. *Biochemistry* **1971**, *10*, 2436), we have developed a new method for analyzing the set of SAXS curves using a global fitting procedure, which allows us to derive the form factor of all the met-myoglobin species present in the solution, their aggregation state, and the set of thermodynamic parameters, with their *p* and *T* dependence. This method also overcomes a reasonably poor quality of the experimental data, and it is found to be very powerful in analyzing SAXS data. SAXS experiments were performed at four different temperatures from hydrostatic pressures up to about 2000 bar. As a result, the presence of an intermediate, partially unfolded, dimeric state of met-myoglobin that forms during denaturation has been evidenced. The obtained parameters were then used to derive the met-myoglobin *p*, *T* phase diagram that fully agrees with the corresponding phase diagram obtained by spectroscopic measurements.

I. Introduction

Despite the large number of studies on the native structure of proteins, folding/unfolding processes remain the object of huge attention. The characterization of conformational transitions and denaturation intermediates is in fact important not only for the determination of the folding pathways but also for the analysis of the principles of protein structure stabilization.[1−4] Moreover, conformational changes are one of the major keys in the regulation of protein activity (see for example ref 5).

In solution, protein denaturation can be induced by changing temperature or solvent composition (e.g., by varying pH or adding denaturants or salts) or by applying external pressure (mechanical or osmotic).[6] Pressure effects are particularly relevant as they are only determined by changes in sample volume that are related to the nature and strength of the hydration forces stabilizing the protein's native conformation.[7] On the other hand, an increasing external pressure lowers the freezing point of the aqueous solution so that the cold-denaturation process,[8] assessed only for a relatively small number of proteins,[9−13] becomes experimentally accessible.

Whether the protein denatured states obtained in different ways are structurally equivalent or different has been a target of many discussions.[6,14,15] It is generally admitted that protein molecules can mainly be in a more or less completely unfolded state in the presence of large concentrations of urea or guanidinium chloride; other denaturing agents (such as temperature, pressure, pH, monohydric alcohols, etc.) would only guide protein molecules into different "partially unfolded'' states.[4,6] Protein association during folding/unfolding is another interesting matter.[16] Molten globule intermediates are known to readily form oligomers,[17,18] and a large tendency to aggregate has been observed for temperature-denatured or partially denatured proteins.[14] On the contrary, pressure is known to favor dissociation of oligomers:[14,19,20] in fact, dissociation is usually observed at about 1−2 kbar, and the unfolding process occurs at around 5 kbar.[19]

As such, proteins in aqueous solutions are stable only in a narrow range of pressure, *p*, and temperature, *T*. A thermodynamic description of the unfolding process has been developed by Hawley in terms of changes in protein heat capacity, thermal expansivity, and compressibility.[21] As a result, an elliptic phase diagram in the *p*, *T* plane that describes at one time the cold-, heat-, as well as pressure-denaturation process has been derived.[14] Hawley's theory is based on the assumption that denaturation is just a two-state transition. However, this point was questioned by several measurements, showing, for a significant number of proteins, the occurrence of an intermediate state.[22−27] Moreover, it has also been suggested that a more complex phase diagram could occur when intermolecular interactions are also taken into account (see for example ref 14). In this case, metastable aggregate protein states appear in the *p*, *T* diagram.

Met-myoglobin is a clear example of this general condition.[12,28] The first met-myoglobin *p*, *T* phase diagram, derived by Zipp and Kauzmann in 1973 by using spectroscopic techniques,[13] turned out to be very similar to Hawley's prediction. The experimental observations indicate that pressure, heat, urea, and acids produce similar structural changes in the vicinity of the met-myoglobin heme group, but no information on global

† Dipartimento di Scienze applicate ai Sistemi Complessi.
‡ Institut für Festkörperforschung.
§ Sincrotrone Trieste.
|| Dipartimento di Fisica.

10.1021/jp063427m CCC: $37.00
Published on Web 03/21/2007

structural changes was obtained. On the other hand, an extended phase diagram that includes both denaturation and aggregation phenomena was reported by Smeller.[14] Basing on infrared measurements, he suggested that the intermediate structure, which occurs during the refolding of pressure-denatured myoglobin, is a destabilized state of the protein that is prone to aggregation.[15] The aggregated state proved to be more stable than the intermediate one, formed during refolding, so that if the aggregate was once formed, e.g., at high temperature, it would also turn out to be stable at room temperature. In this context, a recent report by Gebhardt and co-workers[29] is noteworthy: light scattering experiments evidence an unusual pressure-induced specific and reversible association of native met-myoglobin at low pressure and low pH regimes. The authors suggested that association is controlled by the antagonistic effects of the attractive van der Waals forces, positive volume change upon charge compensation by the phosphate of the buffer (which provides a compensating negative charge), and electrostatic repulsion that occurs in acidic conditions when histidyl residues become protonated. High-pressure enhances the low volume, charged state, favoring the positive protein charge. As a result, at acidic pH and in the pressure range from a few hundreds to a thousand bar, met-myoglobin monomers are in equilibrium with oligomeric particles of low molecular weight (an aggregation number lower than 10 was derived).

To improve the knowledge on structural changes and aggregational phenomena occurring on met-myoglobin during pressure- and temperature-induced denaturation, we performed in solution high-pressure Small-Angle X-ray Scattering (SAXS) experiments. This technique is particularly suitable to study the structural properties of macromolecular systems[4,30−34] even if the data analysis in the case of polydisperse systems (as during the unfolding process, when the protein conformation is not unique) could be very tricky (see for example ref 35). However, we recently showed that global fit approaches, i.e., the simultaneous fit of all the scattering curves based on a suitable physical model, can successfully provide relevant structural and thermodynamical information even for mixed systems.[36,37] Accordingly, an original global fitting method, which integrates both Hawley's thermodynamic approach and structural models for the different protein forms, has been derived to analyze the present SAXS data.

II. Phase Diagram for Protein Denaturation

The thermodynamic analysis of the met-myoglobin denaturation pathway is based on the description of the unfolding process reported by Hawley,[21] which assumes that only two distinct states of the protein, the native, N, and the unfolded, U, exist. Accordingly, the Gibbs free energy difference, $\Delta G = G^{(U)} - G^{(N)}$, can be written in terms of six thermodynamic functions

$$\Delta G(p,T) = \frac{\Delta\beta}{2}(p-p_0)^2 + \Delta\alpha(p-p_0)(T-T_0) - \Delta C_p\left[T\left(\log\frac{T}{T_0} - 1\right) + T_0\right] + \Delta V_0(p-p_0) - \Delta S_0(T-T_0) + \Delta G_0 \quad (1)$$

where $\beta = (\partial V/\partial p)_T$ is the protein compressibility factor (V being the protein volume), $\alpha = (\partial V/\partial T)_p$ the thermal expansivity factor, C_p the heat capacity, and ΔV_0, ΔS_0, and ΔG_0 are the changes in protein volume, entropy, and free energy at the N to U transition calculated at the reference pressure and temperature, p_0, and T_0 (hereafter, $p_0 = 1$ bar and $T_0 = 273.15$ K; note also that, in the symbols used for the variables that are functions of p and T, this dependence is no more indicated). In the Hawley approach, β, α, and C_p are considered constant with p and T, being their values characteristic for the N and U states. In the p, T plane, the transition contour, corresponding to the condition $\Delta G = 0$, has a pseudo-conic shape and, as said by Smeller,[14] "always for proteins was found to be elliptic''.

If an intermediate, possibly oligomeric state (I) occurs during denaturation,[14,38] two possible transitions should now be considered: $N \rightarrow (1/a_I)I$ and $N \rightarrow U$ (the average aggregation number for the intermediate state, a_I, has been introduced to take into account possible aggregate forms[14,29]). The corresponding equilibrium constants, which can be defined in terms of molar fraction x_i of the i-th species and of the total molar monomer concentration c, are

$$K_{NI} = e^{-\Delta G^{(NI)}/k_B T} = \frac{x_I^{1/a_I}}{a_I^{1/a_I} c^{1-1/a_I} x_N}$$
$$K_{NU} = e^{-\Delta G^{(NU)}/k_B T} = \frac{x_U}{x_N} \quad (2)$$

where the free energy differences, $\Delta G^{(NI)} = (1/a_I)G^{(I)} - G^{(N)}$ and $\Delta G^{(NU)} = G^{(U)} - G^{(N)}$, can be described according to eq 1 using the corresponding set of thermodynamic parameters.

One point should be stressed. The "protein volume'' here considered refers to the partial molar protein volume, $V = (\partial V_{sol}/\partial n)_{p,T}$, where V_{sol} is the volume of the solution and n is the number of protein moles added to the solution. This volume is known as "displaced volume'', because it represents the change in the solution volume after the addition of a small amount of solute. It should be clear that it differs from the intrinsic protein volume ("core volume'', V_C) because it includes the solvent interaction effects on the protein volume ("interaction volume'', V_{int}); in particular,

$$V = V_C + V_{int} \quad (3)$$

As β and α are considered constant,[21] the displaced volume is a linear function of p and T. Assuming that the core volume also shows the same behavior, we can write (i = N, I, and U):

$$V^{(i)} = a_i M_1[v_0^{(i)} + \hat{\beta}^{(i)}(p-p_0) + \hat{\alpha}^{(i)}(T-T_0)]$$
$$V_C^{(i)} = a_i M_1[v_{0C}^{(i)} + \hat{\beta}_C^{(i)}(p-p_0) + \hat{\alpha}_C^{(i)}(T-T_0)] \quad (4)$$

where M_1 is the monomer molecular weight and $v_0^{(i)}$, $v_{0C}^{(i)}$, $\hat{\beta}^{(i)}$, $\hat{\beta}_C^{(i)}$, $\hat{\alpha}^{(i)}$, and $\hat{\alpha}_C^{(i)}$ are the standard volume, the compressibility factor, and the thermal expansion factor per unit mass of the protein in the i-th state for the displaced and the core volumes, respectively.

III. Protein Scattering Model

In general, the observable quantity in a SAXS measurement is the macroscopical differential scattering cross section, $d\Sigma/d\Omega(Q) = (c/N_A)\,P(Q)\,S(Q)$ as a function of the scattering vector $\mathbf{Q}$ ($Q = 4\pi \sin\theta/\lambda$, 2θ being the scattering angle, λ the X-ray wavelength, and N_A Avogadro's number). For isotropic systems, $P(Q)$ is the effective form factor, depending on the shape, size, and distribution of the protein conformers in solution and $S(Q)$ is the effective structure factor, depending on the protein−protein interactions.[36] For dilute protein solutions ($c < 10^{-5}$ M), the structure factor is negligible ($S(Q) \approx 1$) and the measured SAXS cross section only depends on the form factor.

According to the protein denaturation pathway, the effective form factor of met-myoglobin is given by the superposition of

the form factors $P_N(Q)$, $P_I(Q)$, and $P_U(Q)$ of the three different states present in solution:

$$P(Q) = x_N P_N(Q) + \frac{x_I}{a_I} P_I(Q) + x_U P_U(Q) \quad (5)$$

The form factor of the met-myoglobin in the native state has been calculated from the crystallographic structure in the Protein Data Bank, 4MBN.[28] Technical details on the Monte Carlo calculation can be found in refs 36, 39, and 40: the resulting protein core volume is $V_C^{(pdb)} = 13\,200 \pm 200$ cm^3 mol^{-1}, and the protein hydration shell volume (the thickness of the layer around the protein has been fixed to 3 Å)[40] is $V_H^{(pdb)} = 7600 \pm 200$ cm^3 mol^{-1}. The calculation of $P_N(Q)$ as a function of p and T makes use of the following assumptions: (i) the core volume $V_C^{(N)}$ is a linear function of p and T (eq 4), and the same function is used for approximating the hydration volume $V_H^{(N)} = V_C^{(N)} V_H^{(pdb)}/V_C^{(pdb)}$; (ii) the protein shape does change only isotropically with p and T; (iii) the interaction volume $V_{int}^{(N)}$ in eq 3 does not coincide with the hydration shell volume $V_H^{(N)}$, but it can be written as $V_{int}^{(N)} = -V_H^{(N)}(\rho_H^{(N)} - \rho_B)/\rho_B$, ρ_H and ρ_B being the scattering length density of the water in the hydration shell and in the bulk, respectively.

By defining the three protein partial form factors $P_{CC}(Q)$ (the core term), $P_{HH}(Q)$ (the shell term), and $P_{CH}(Q)$ (the cross term) via the Fourier transform of the distance distribution functions $p_{CC}(r)$, $p_{HH}(r)$, and $p_{CH}(r)$ estimated by the Monte Carlo multi-density method, the effective form factor can be written as[41]

$$P_N(Q) = (\rho_C^{(N)} - \rho_B)^2 (V_C^{(N)})^2 P_{CC}(Q\gamma^{1/3}) + (\rho_H^{(N)} - \rho_B)^2 (V_H^{(N)})^2 P_{HH}(Q\gamma^{1/3}) + 2(\rho_C^{(N)} - \rho_B)(\rho_H^{(N)} - \rho_B) V_C^{(N)} V_H^{(N)} P_{CH}(Q\gamma^{1/3}) \quad (6)$$

where $\rho_C^{(N)}$ is the scattering length density of the protein core and $\gamma = V_C^{(N)}/V_C^{(pdb)}$.

For what concerns the denaturated states, the worm-like chain form factor, developed by Pedersen and Schurtenberger,[4,37,42] has been used. To describe the structure of the protein chain with a finite, circular section of radius $R_C^{(D)}$ and a hydration shell of $\delta = 3$ Å, this form factor has been multiplied by the cross-section function $S_{sc}(Q)$,

$$S_{sc}(Q) = 4\pi^2 L^2 \left[(\rho_C^{(D)} - \rho_H^{(D)})(R_C^{(D)})^2 \frac{J_1(QR_C^{(D)})}{QR_C^{(D)}} + (\rho_H^{(D)} - \rho_B)(R_C^{(D)} + \delta)^2 \frac{J_1(Q(R_C^{(D)} + \delta))}{Q(R_C^{(D)} + \delta)} \right]^2 \quad (7)$$

where L is the contour length of the full chain and $J_1(x)$ is the first order Bessel function. In this case, the p and T dependence of the statistical segment (Kuhn) length b of the number of statistical segments n_b, such as $n_b b = L$, is expressed as follows:

$$b^{(D)} = b_0^{(D)} + \beta_b^{(D)}(p - p_0) + \alpha_b^{(D)}(T - T_0)$$
$$n_b^{(D)} = n_{b_0}^{(D)} + \beta_{n_b}^{(D)}(p - p_0) + \alpha_{n_b}^{(D)}(T - T_0) \quad (8)$$

where $b_0^{(D)}$, $n_{b_0}^{(D)}$, $\beta_b^{(D)}$, $\beta_{n_b}^{(D)}$, $\alpha_b^{(D)}$, and $\alpha_{n_b}^{(D)}$ are the reference values, pressure dependence coefficient, and temperature dependence coefficient of b and n_b, respectively, for each of the denaturated states. Combining simple geometrical relationships and eqs 4 and 8, the p, T dependence of $R_C^{(D)}$ and $V_H^{(D)}$ can be derived.

The behavior of $d\Sigma/d\Omega(Q)$ at small Q can also provide evidence of the protein states. Two distinct approximations, i.e., the Guinier and Debye laws,[34,43,44] which are valid for compact and unfolded protein conformations, respectively, allow the calculation of the scattering cross section at zero angle, $d\Sigma/d\Omega(0)$, and the average gyration radius R_g. A comparison of the results obtained with these two approximations will help to have a clearer picture of the system.

IV. Materials and Methods

A. Sample Preparation and SAXS Measurements. Met-myoglobin (type III myoglobin from horse heart, salt free, iron present in ferric state) was obtained from Sigma (St. Louis, MO) (99% purity) and used without further purification. Samples were prepared by dissolving the dry powder in acetate buffer 50 mM (pH 4.5). The final protein concentration was adjusted to 10 mg/mL.

Small-angle X-ray scattering experiments were performed at the SAXS beam-line at ELETTRA Synchrotron (Trieste, Italy) with $\lambda = 1.54$ Å and $0.035 < Q < 0.2$ Å^{-1}. For high-pressure experiments, we used the pressure-control system designed and constructed by M. Kriechbaum and M. Steinhart.[45] The pressure cell has two diamond windows (3.0 mm diameter and 1 mm thickness) and allowed us to measure scattering patterns at hydrostatic pressures of up to ~2000 bar. Particular care was taken to check for radiation damage and for equilibrium conditions. In test experiments, measurements were repeated several times at the same constant pressure and temperature to account for stability of the scattering profiles. Accordingly, exposure times of few seconds were chosen to obtain a sufficient signal-to-noise ratio and to limit the radiation damage. SAXS patterns were collected as a function of pressure at temperatures of 10, 20, 30, and 45 °C. The SAXS experimental intensities were corrected for background, buffer contributions, detector inhomogeneities, and sample transmission. Unfortunately, no calibration of the experimental data was available.

B. Model Parameters and Best-Fit Analysis. Due to low protein concentration and use of the high-pressure cell, the quality of experimental data was poor and not comparable to what in general is obtained with a standard synchrotron SAXS apparatus. In particular, our samples did show low scattering power, comparable to the parasitic scattering of the cell. For this reason, we resorted to a global fit procedure, which provided excellent results even in the presence of poor data.[37] From a qualitative point of view, the fit procedure combines the form factors for the N, U, and I states to simultaneously reproduce all the experimental scattering curves. In the data analysis, a thermodynamic relationship binds the composition of met-myoglobin in different forms with pressure and temperature; the N, U, and I protein form factors are dependent on p and T and on the characteristics of the hydration shell, which also alter with p and T; the intermediate state is allowed to be oligomeric.

The physical model therefore includes 23 parameters related to the thermodynamic description, 12 related to the form factors of the different protein states, and 1 that refers to the experimental data calibration. The full set of parameters has been described below.

The thermodynamic parameters are as follows: a_I is the aggregation number of the I state; for the two N − I and N − U transitions, the parameters are the reference Gibbs free energy differences $\Delta G_0^{(NI)}$ and $\Delta G_0^{(NU)}$; the reference entropy differ-

TABLE 1: Parameters Obtained by the Global Fitting Procedure Applied to the 53 Experimental SAXS Curves

parameter	units	range of validity	refs	notes	result
κ	au cm				4.58 ± 0.02
a_I					2.02 ± 0.08
$\Delta G_0^{(NI)}$	kcal mol^{-1}	$-8 \div 8$	13, 14, 21, 25, 50−53	*a*	-3.81 ± 0.09
$\Delta S_0^{(NI)}$	cal mol^{-1} K^{-1}	$-500 \div 500$	53	*b*	-43 ± 9
$\Delta C_p^{(NI)}$	cal mol^{-1} K^{-1}	$0 \div 3000$	25	*c*	20 ± 10
$\Delta V_0^{(NI)}$	cm^3 mol^{-1}	$-200 \div -1$	13		-60 ± 20
$\Delta\hat{\beta}^{(NI)}$	10^{-6} cm^3 g^{-1} bar^{-1}	$-7 \div 4$	49	*d*	-1.3 ± 0.7
$\Delta\hat{\alpha}^{(NI)}$	10^{-5} cm^3 g^{-1} K^{-1}	$-7 \div 7$	54		-2 ± 2
$\Delta G_0^{(NU)}$	kcal mol^{-1}	$1 \div 8$	13, 14, 21, 25, 50−53	*a*	2.4 ± 0.3
$\Delta S_0^{(NU)}$	cal mol^{-1} K^{-1}	$-500 \div 500$	53	*b*	-192 ± 7
$\Delta C_p^{(NU)}$	cal mol^{-1} K^{-1}	$2000 \div 3000$	13		2400 ± 80
$\Delta V_0^{(NU)}$	cm^3 mol^{-1}	$-200 \div -1$	13		-80 ± 20
$\Delta\hat{\beta}^{(NU)}$	10^{-6} cm^3 g^{-1} bar^{-1}	$-20 \div -3$	49	*d*	-3.3 ± 0.3
$\Delta\hat{\alpha}^{(NU)}$	10^{-5} cm^3 g^{-1} K^{-1}	$-7 \div 7$	54		-5 ± 2
$\hat{\beta}^{(N)}$	10^{-6} cm^3 g^{-1} bar^{-1}	$-12 \div -1$	54		-1.7 ± 0.4
$\hat{\alpha}^{(N)}$	10^{-5} cm^3 g^{-1} K^{-1}	$3 \div 10$	54		5 ± 1
$\hat{\beta}_C^{(N)}$	10^{-6} cm^3 g^{-1} bar^{-1}	$-13 \div -7$	55		-8.604 ± 0.002
$\hat{\alpha}_C^{(N)}$	10^{-5} cm^3 g^{-1} K^{-1}	$3 \div 12$	54		10.0 ± 0.4
$v_{0C}^{(I)}$	cm^3 g^{-1}	$0.755 \div 0.776$	13		0.7750 ± 0.0004
$\hat{\beta}_C^{(I)}$	10^{-6} cm^3 g^{-1} bar^{-1}	$-13 \div -7$	49		-8.604 ± 0.007
$\hat{\alpha}_C^{(I)}$	10^{-5} cm^3 g^{-1} K^{-1}	$3 \div 12$	54		10.0 ± 0.3
$v_{0C}^{(U)}$	cm^3 g^{-1}	$0.755 \div 0.776$	13		0.7749 ± 0.0002
$\hat{\beta}_C^{(U)}$	10^{-6} cm^3 g^{-1} bar^{-1}	$-13 \div -7$	49		-8.60 ± 0.03
$\hat{\alpha}_C^{(U)}$	10^{-5} cm^3 g^{-1} K^{-1}	$3 \div 12$	54		10.0 ± 0.4
$b_0^{(I)}$	Å	$4 \div 100$		*e*	40 ± 10
$n_{b_0}^{(I)}$		$2 \div 153$		*f*	4 ± 1
$\beta_b^{(I)}$	10^{-4} Å bar^{-1}	$-20 \div -1$		*g*	-2 ± 1
$\beta_{n_b}^{(I)}$	10^{-4} bar^{-1}	$-10 \div -1$		*g*	-4 ± 3
$\alpha_b^{(I)}$	10^{-3} Å K^{-1}	$1 \div 10$		*g*	6 ± 3
$\alpha_{n_b}^{(I)}$	10^{-3} K^{-1}	$0.1 \div 10$		*g*	1.1 ± 0.5
$b_0^{(U)}$	Å	$4 \div 153$		*e*	8 ± 2
$n_{b_0}^{(U)}$		$2 \div 153$		*f*	20 ± 10
$\beta_b^{(U)}$	10^{-4} Å bar^{-1}	$-20 \div -1$		*g*	-2 ± 1
$\beta_{b_0}^{(U)}$	10^{-4} bar^{-1}	$-10 \div -1$		*g*	-2.0 ± 0.8
$\alpha_b^{(U)}$	10^{-3} Å K^{-1}	$1 \div 10$		*g*	5 ± 2
$\alpha_{n_b}^{(U)}$	10^{-3} K^{-1}	$0.1 \div 10$		*g*	1.0 ± 0.7

[a] The range reported in literature has been enlarged as the unfolded or intermediate states could be oligomeric. [b] Values could be positive or negative, depending on the eventual aggregation during unfolding. [c] If the I state preserves many secondary structure elements of the native state (and maybe also a fraction of the tertiary structure), $\Delta C_p^{(NI)}$ is expected to be rather small; on the contrary, if the intermediate state is more similar to the unfolded state, $\Delta C_p^{(NI)}$ would be big. [d] Chalikian and Breslauer[49] found that the transition from the N to I state is accompanied by a small increasing $\hat{\beta}$, and at the N to U transition, the change is large and negative. However, they also partially describe unfolded states, characterized by a small and negative changing $\Delta\hat{\beta}$. Considering these observations, we defined the range of $\Delta\hat{\beta}^{(NI)}$ making both negative or positive variations possible, and the range of $\Delta\hat{\beta}^{(NU)}$ was only negative. [e] It should not be lower than a typical distance between two amino-acids; the upper limit cannot overcome the full protein chain length. [f] It should be between 2 and the total number of amino-acids of the met-myoglobin chain, eventually multiplied by the aggregation number a_D. [g] The range has been selected to avoid very large variations within the $(p - T)$ plane, which would not be compatible with the assumption of two equilibria between three nearly distinct protein states.

ences are $\Delta S_0^{(NI)}$ and $\Delta S_0^{(NU)}$; the reference protein volume differences are $\Delta V_0^{(NI)}$ and $\Delta V_0^{(NU)}$; the heat capacity differences are $\Delta C_p^{(NI)}$ and $\Delta C_p^{(NU)}$; the compressibility factors per unit mass differences are $\Delta\hat{\beta}^{(NI)}$ and $\Delta\hat{\beta}^{(NU)}$; and the thermal expansion factors per unit mass differences are $\Delta\hat{\alpha}^{(NI)}$ and $\Delta\hat{\alpha}^{(NU)}$. For the native N state, the parameters are as follows: compressibility factors per unit mass for displaced and core volumes are $\hat{\beta}^{(N)}$ and $\hat{\beta}_C^{(N)}$, and thermal expansion factors per unit mass for displaced and core volumes are $\hat{\alpha}^{(N)}$ and $\hat{\alpha}_C^{(N)}$. For intermediate, I, and unfolded, U, states the parameters are as follows: standard core volumes per unit mass are $v_{0C}^{(I)}$ and $v_{0C}^{(U)}$; compressibility factors per unit mass for core volumes are $\hat{\beta}_C^{(I)}$ and $\hat{\beta}_C^{(U)}$; and thermal expansion factors per unit mass for core volumes are $\hat{\alpha}_C^{(I)}$ and $\hat{\alpha}_C^{(U)}$.

The protein form factor of the I and U states depends on the following unknown 12 parameters: two reference statistical segment (Kuhn) lengths, $b_0^{(I)}$ and $b_0^{(U)}$; two reference numbers of statistical segments, $n_{b_0}^{(I)}$ and $n_{b_0}^{(U)}$; two pressure-dependent coefficients, $\beta_b^{(I)}$ and $\beta_b^{(U)}$ of $b^{(I)}$ and $b^{(U)}$; two pressure-dependent coefficients, $\beta_{n_b}^{(U)}$ and $\beta_{n_b}^{(I)}$ of $n_{b_0}^{(I)}$ and $n_{b_0}^{(U)}$; two

temperature-dependent coefficients, $\alpha_b^{(I)}$ and $\alpha_b^{(U)}$ of $b^{(I)}$ and $b^{(U)}$; and two temperature-dependent coefficients, $\alpha_{n_b}^{(U)}$ and $\alpha_{n_b}^{(I)}$ of $n_{b_0}^{(I)}$ and $n_{b_0}^{(U)}$.

Finally, due to the missing calibration of the experimental data, a further parameter has been introduced, the calibration factor κ, which is common to all the experimental curves measured in a single instrumental configuration. This factor transforms the experimental intensities into scattering cross sections in absolute units by comparing the experimental and theoretical intensities.

As expected, the choice for the range of validity of the fitting parameters is a crucial part of this work, and they are all shown in Table 1 together with proper references. However, a few comments can be reported here. First, published data for the native displaced specific reference volume, $v_0^{(N)}$, show a nearly constant value for all the globular proteins. Because small changes do not affect fitting results, we fixed $v_0^{(N)}$ to the standard value[46] of 0.71 cm^3 g^{-1}. Second, a very small sensitivity of the final results on the native core specific reference volume, $v_{0C}^{(N)}$, was found. Therefore, we fixed it to the value found by the Monte Carlo method, namely $v_{0C}^{(N)} = V_C^{(pdb)}/M_1 \equiv 0.78$ cm^3 g^{-1}.

The 36 unknown parameters enable the calculation of a model scattering cross section $[d\Sigma/d\Omega](Q)$ at any p and T and compare them with the experimental data. We applied a global fit procedure based on the contemporaneous analysis of the whole set of the experimental SAXS curves. The global merit functional to be minimized is defined in ref 36. The method used to optimze the unknown parameters is the simulated annealing as explained in ref 47. It should be noticed that the large number of fitting parameters (36) is not a weak aspect of the proposed method. In fact, 53 SAXS curves, for a total of about 1500 Q-data points, have been globally analyzed, i.e., less than one parameters per curve. The effect of experimental uncertainties on the fitting parameters was determined using a sampling method as explained in ref 36.

Some experimental data (namely those at the highest p and T) do show a weak interference peak at the very low Q region, i.e., at $Q < 0.055$ Å^{-1}. Because the analysis of protein−protein interactions remains out of the aim of the present work, we have neglected points only for those curves where the interference effect was present.

V. Results

53 SAXS measurements were performed on a met-myoglobin solution at the concentration of 10 g L^{-1} in 50 mM buffer acetate at pH 4.5 as a function of temperature and mechanical pressure. The measurements were performed at different fixed temperatures by increasing the pressure from 1 up to about 2000 bar. Few SAXS curves at 20 °C are reported in Figure 1. Despite the missing calibration of the experimental data, the values are shown in absolute units by using the common calibration factor κ of the global fit.

The whole set of SAXS data in the form of Kratky plots[31,32] is shown in Figure 2. It can be observed that the large peak that centers at about 0.1 Å^{-1} (which indicates the presence of a globular native state) tends to broaden and then to disappear at the highest temperatures and/or pressures. This is a first confirmation that high-pressure SAXS marks the pressure-assisted and heat denaturation processes of met-myoglobin.

At first, to evaluate the structural differences among the various thermodynamic conditions, the radius of gyration of the scattering particles has been determined as a function of p and T by Guinier (valid for compact particles) and Debye (valid for unfolded chains) approximations. Results are plotted in Figure 3 (note that errors on R_g and $[d\Sigma/d\Omega](0)$ are quite big, of the order of 10%, due to the high experimental uncertainties at low Q, which are detected with the high-pressure setup).

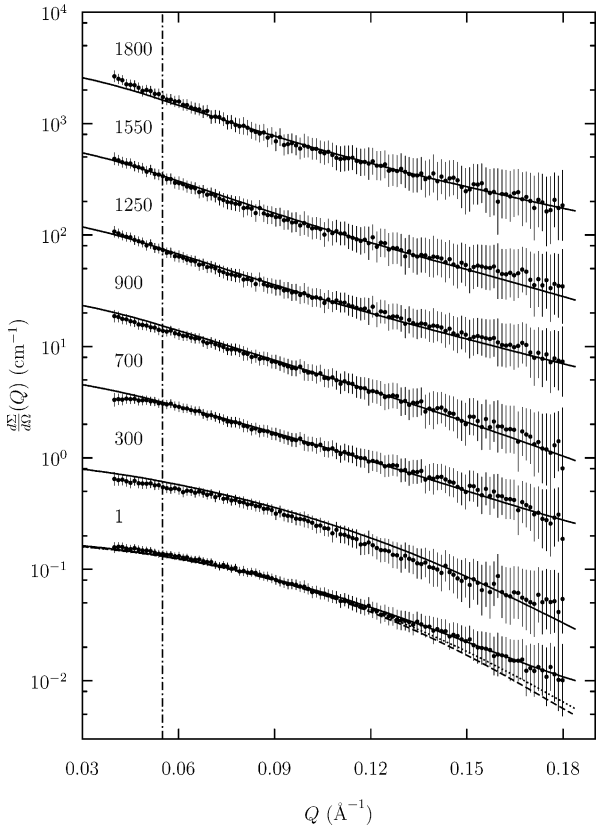

Figure 1. Semilogarithmic SAXS patterns of a solution of met-myoglobin at concentration of 10 g L^{-1} in a 50 mM acetate buffer, pH 4.5, temperature 20 °C, and at various pressures (values indicated in bar at the top of each curve). Solid lines are the best fitting curves obtained by the global fit analysis. Bottom dashed line: form factor of the met-myoglobin calculated by the CRYSOL tool. Bottom dotted line: form factor obtained with the Monte Carlo tool. For both CRYSOL and Monte Carlo methods, the protein water shell thickness is 3 Å and its contrast with respect to the bulk water is 0.0168 10^{-12} cm Å^{-3}. The vertical dotted line indicates the low Q-limit considered in the fitting procedure.

At ambient temperature and pressure, the value obtained using the Guinier approximation is 17 ± 1 Å, in good agreement with the value calculated from the crystallography coordinates. This confirms that at ambient conditions met-myoglobin is in the native state. At all the investigated temperatures, the radius of gyration shows a trend with pressure, slightly increasing up to ∼1500 bar, and then reaching almost a constant value. It is found that the R_g values calculated with the Debye approximation (within the range $Q < 3/R_g$) are systematically higher than those calculated by using the Guinier law. In particular, at the higher investigated p, the difference between Guinier and Debye R_g becomes very large, but it should be noticed that the number of points in the Guiner range ($Q < 1.3/R_g$) is rather small, which reflects larger uncertainty. The observed pressure dependence of R_g confirms the presence of a transition pathway that is different at each investigated temperature.

This is also confirmed by the $d\Sigma/d\Omega(0)$ values, which, at high pressure and/or temperature, are found to be about a factor of 2 larger than those values found at ambient pressure and temperature. This value of 2 indicates that in solution oligomeric structures larger than dimers would not be present.

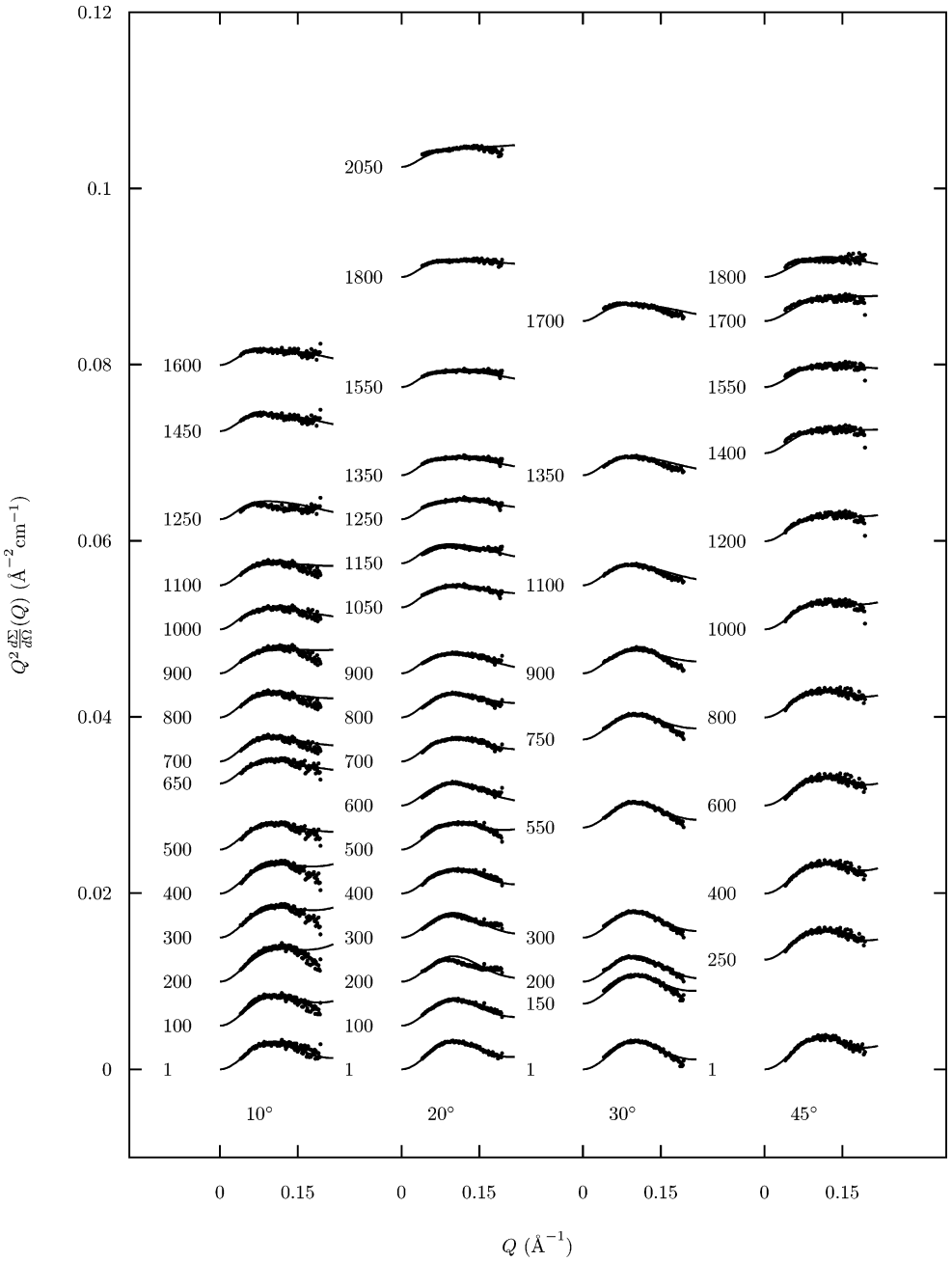

Figure 2. Kratky plots of SAXS data collected at different temperatures (reported in degrees Celsius below each column of curves) and pressures (values indicated in bar at the left of each curve). Solid lines are the best fitting curves obtained by the global fit analysis. For the sake of clarity, the factor $5 \times 10^{-5}(p - 1)$ (p is in bar) has been added to each curve.

SAXS curves were then analyzed using the best-fit procedure described in Section IV.B. At first, it was observed that the form factor for native met-myoglobin, calculated by using the CRYSOL software,[39] agrees with data obtained at $p = 1$ bar and $T = 20$ °C. The comparison is reported in the bottom curve of Figure 1 and confirms that in these experimental conditions met-myoglobin is in its native state. The same data were then analyzed using the Monte Carlo method introduced in Section III: the fitted form factor, calculated using the same contrast $\rho_H - \rho_B = 0.0168 \times 10^{-12}$ cm Å^{-3} found by CRYSOL and using the van der Waals envelope volume, $V_C^{(pdb)} = 13\,200 \pm 200$ cm^3 mol^{-1} and hydration shell volume, $V_H^{(pdb)} = 7600 \pm 200$ cm^3 mol^{-1}, is also shown in Figure 1 to emphasize the quality of the Monte Carlo procedure.

Global fit analysis was then performed by leaving all the thermodynamic and structural parameters free to vary in the ranges defined in Table 1. The final merit functional was $\chi^2 = 0.16$. The best fit curves were superimposed on the experimental data in Figures 1 and 2. Therefore, the quality of the fit is very good.

VI. Discussion and Conclusions

In-solution small-angle X-ray scattering has been used to analyze the met-myoglobin during temperature and pressure-induced denaturation processes at pH 4.5. As shown in Figures 1 and 2, scattering profiles present a clear dependence on p and T.

A first analysis has been performed considering the changes in the radius of gyration and in the intensity scattered at zero

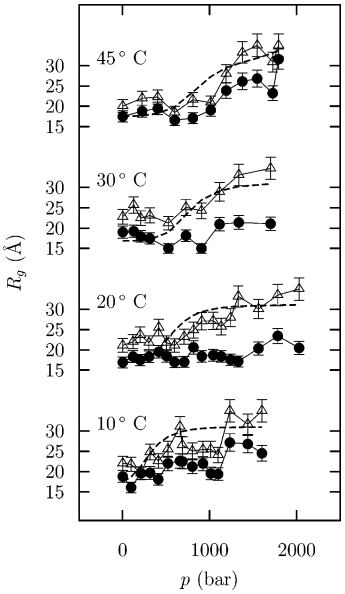

Figure 3. Plot of the radii of gyration obtained by applying the Guinier (circles) and the Debye (triangles) approximations to the experimental SAXS curves. Dashed lines refer to the R_g values calculated from the $p(r)$ functions obtained by the global fit analysis.

angle: although data reported in Figure 3 suggest that structural transitions occur as a function of pressure and temperature, the $[d\Sigma/d\Omega](0)$ values obtained in the different experimental conditions clearly indicate that aggregation states larger than dimers are not present.

Despite the poor quality of the experimental data, due to the fact that the parasitic scattering of the pressure cell was comparable to the sample scattering, the 53 SAXS curves were then analyzed by using the original global fitting method (36 fitting parametrs with about 1500 experimental points) described in Section IV.B, which integrates Hawley's approach and structural models for the different protein states (see Section III). In particular, three different states, namely the native, an intermediate form (eventually oligomeric), and the unfolded, have been considered to occur during the unfolding process. Although the native state has been described using the met-myoglobin crystallographic structure, both the intermediate and unfolded states were conveniently represented using the worm-like model. The global fitting analysis was performed considering that all the thermodynamic and structural parameters are free to vary in the ranges defined in Table 1. The obtained curves are superimposed to the data in Figures 1 and 2; Table 1 shows the best-fit global parameters.

A few technical points need short commenting. First, a unique scaling factor κ was fitted with a relativing low uncertainty ($\kappa = 4.58 \pm 0.02$ au cm), confirming the quality of SAXS data reduction. Second, the correlation matrix (not shown) indicates that all parameters (with the unique exception of the compressibility and thermal expansivity factors for the I and U states, which show a degree of correlation of about 40%) are uncorrelated, confirming the general goodness of both the adopted model and chosen ranges of validity of the parameters. The resulting distance distribution functions $p(r)$ (not reported) do indeed show in some cases (at high pressure and/or temperature) non-negligible values up to about 100 Å, which correpond to a first Shannon channel $Q_1 = \pi/D_{max} = 0.03$ Å^{-1},[48] which is lower than the minimun Q considered in the analysis (0.055 Å^{-1}). This confirms that, for most denatured states, the experimental

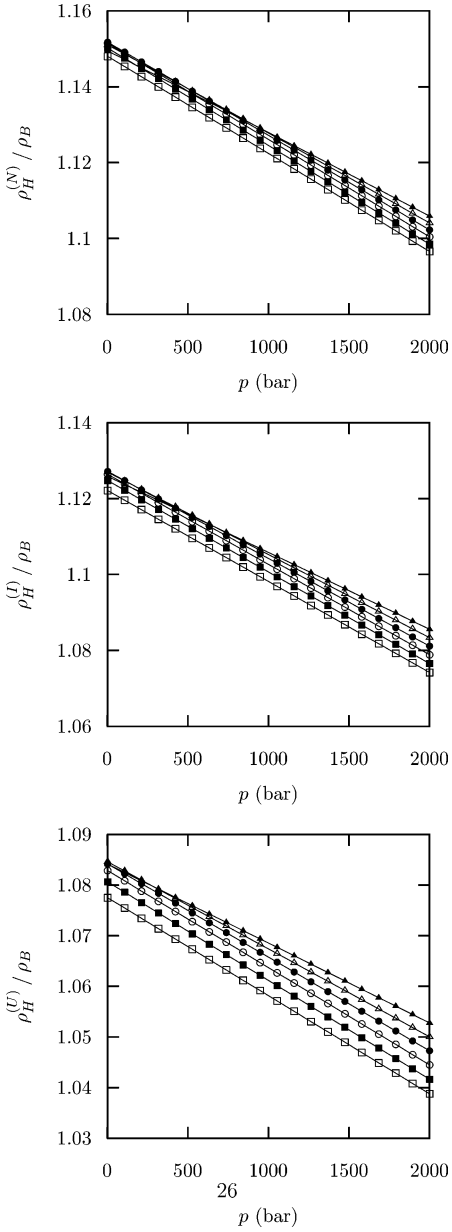

Figure 4. Relative mass density of the protein hydration shell for N, I, and U states of met-myoglobin at pH 4.5 as a function of p for different temperatures: filled triangles, 10 °C; open triangles, 20 °C; filled circles, 30 °C; open circles, 40 °C; filled squares, 50 °C; open squares, 60 °C.

Q-windows are not ideal for one single SAXS curve analysis, although not all the experimental curves do indeed show aggregation.

Nevertheless, the global fit of all the curves together with the constraint of optimizing a unique calibration factor κ enable us to recover the aggregational and/or the conformational properties also from the SAXS curves of denatured states. It is anyway interesting to note in Figure 3 that at low pressure the R_g values are in agreement with those obtained using the Guinier law, and at high pressure, they coincide with those calculated using the Debye approximation, confirming the occurrence of unfolded states.

Direct structural information on different met-myoglobin conformers occurring as a function of p and T can be obtained from the analysis of the corresponding form factors. It can be first observed that the derived form factors strongly depend on the ratio between shell water scattering length density, $\rho_H^{(i)}$, and

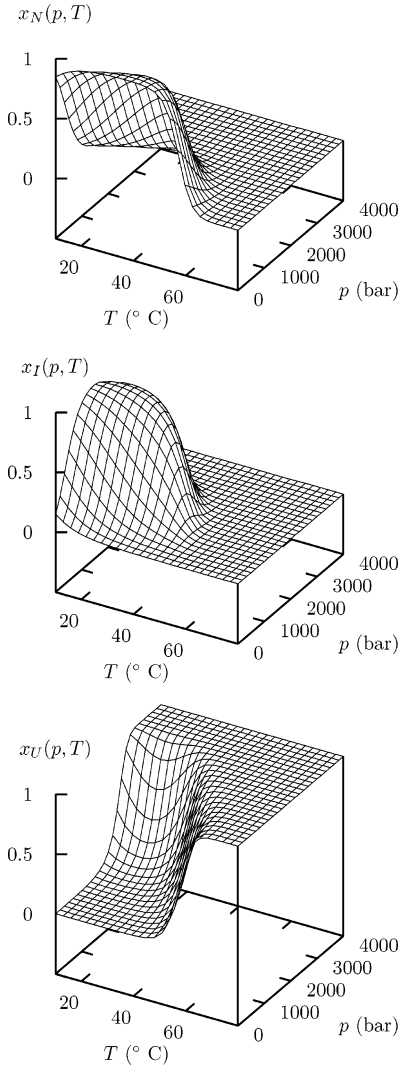

Figure 5. Three-dimensional plots of the molar fractions of the native (x_N), the intermediate (x_I), and the unfolded (x_U) state of the met-myoglobin calculated with the parameters obtained by the global fit of the SAXS curves (Table 1).

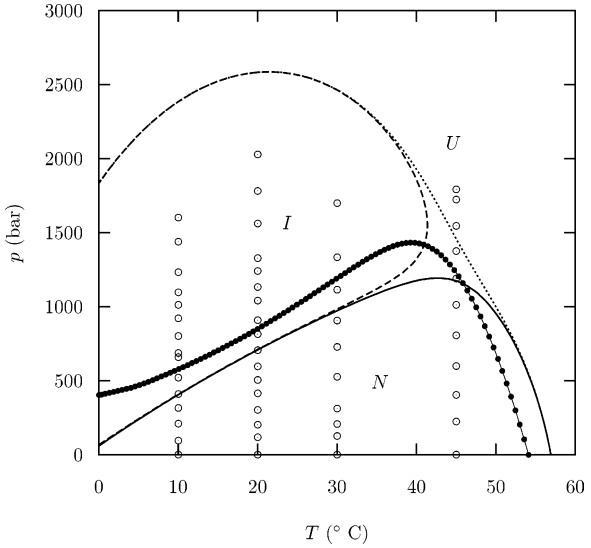

Figure 6. Contours at constant x_i for the denaturation of met-myoglobin at pH 4.5. $x_N = 0.5$, solid line; $x_I = 0.5$, dashed line; $x_U = 0.5$, dotted line. Open circles represent p, T points investigated by the present SAXS experiments. The curve marked with filled circles is the denaturation contour obtained by Zipp and Kauzmann at pH 4.[13]

bulk water scattering length density, ρ_B (i.e., on the shell relative mass density). The $\rho_H^{(i)}/\rho_B$ ratios for the three met-myoglobin states are plotted in Figure 4 as a function of pressure: in all cases, the ratios decrease by increasing both pressure and temperature. Moreover, although the values for the N and I states are higher than 1.00 (ranging from about 1.15 to 1.10 and from about 1.12 to 1.08 in the N and I states, respectively), in the U state, the ratio falls in a lower range, from about 1.08 to 1.04, indicating that a completely different protein surface is exposed to the solvent. Note that for the N and I states the shell relative mass densities are in good agreement with typical values reported by Svergun et al.,[40] and the result obtained in the U state instead is very interesting, as it is not yet clear how unfolded proteins interact with the solvent and how p and T could change this interaction.[25]

Concerning the structure of the two unfolded states, it it is important to point out that the intermediate met-myoglobin state is dimeric ($a_I = 2.02 \pm 0.08$). Moreover, it should also be observed that pressure and temperature dependence coefficients ($\beta_b^{(I)}$, $\beta_{n_b}^{(I)}$, $\alpha_b^{(I)}$, $\alpha_{n_b}^{(I)}$ and $\beta_b^{(U)}$, $\beta_{n_b}^{(U)}$, $\alpha_b^{(U)}$, $\alpha_{n_b}^{(U)}$; see Table 1) are quite similar and rather small (even if they are affected by large uncertainties), even though large differences occur between the parameters that describe the worm-like structures. In particular, for the I state, the contour length was about 180 Å, and the core protein radius was about 8.8 Å; for the U state, the values became 2850 and 1.56 Å, respectively. Moreover, the reference number of statistical segments in the I state is quite small ($n_{b_0}^{(I)} = 4 \pm 1$), and the number is much higher in the U state ($n_{b_0}^{(U)} = 20 \pm 10$). These parameters suggest that the intermediate met-myoglobin form, dimeric, is rather compact and it may be considered a molten globule state. On the other hand, the U state is characterized by a large degree of unfolding.

Among the fitted parameters shown in Table 1, the following points are worthy of discussion: (i) the reference free energy differences are negative and positive for the N − I and N − U transitions, respectively; the positive value confirms the association phenomena occurring at the N − I transition; (ii) the reference entropy differences are negative for both N − I and N − U transitions; the larger negative value at the N − U transition reflects the large degree of disorder of the system in the U state; (iii) $\Delta C_p^{(NU)}$ is in good agreement with the literature data,[13] and the heat capacity change at the N − I transition is much smaller, emphasizing that a large structural similarity characterizes the N and I states;[25] (iv) both changes in compressibility factors $\Delta\hat{\beta}^{(ND)}$ and the reference displaced volume $\Delta V_0^{(ND)}$ do indeed show higher values for the N − U transition than for the N − I one, confirming that the intermediate state is much more compact than the unfolded one.

Therefore, the thermodynamic parameters obtained from the global fit procedure confirm that the intermediate state, which forms during compression, is rather different from the completely unfolded one. Indeed, data suggest that the intermediate state is a destabilized, compact state, in some way similar to the native met-myoglobin conformation, but prone to aggregation.

The global fitting procedure also gives the amount of the different met-myoglobin states occurring in solution in the different experimental conditions. The corresponding molar fractions are shown in Figure 5 as two-dimensional surface functions of p and T. It can be observed that at $p > 3000$ bar only the U state exists at all temperatures. On the other hand, the I state occurs at intermediate pressures, in a rather narrow range, but disappears for $T > 50$ °C. Therefore, no association should be observed either during heat denaturation process at

ambient pressure (or close to ambient) or at pressures higher than about 2 kbar or during the pressure denaturation process performed at high temperature.

The final p, T phase diagram is reported in the form of contour plots of $x_i = 0.5$ in Figure 6. To illustrate the very good agreement, the phase diagram obtained by Zipp and Kauzmann[13] at pH 4 is superimposed. It is worth noticing that the curve derived here is not elliptic, although it has been obtained in the general framework of Hawley's theory.[21] This is due to the presence of an intermediate (and dimeric) protein state: as expected, a more complex diagram is obtained as intermolecular interactions are taken into account.[14] It should be observed that the presence of dimers contrasts with the general finding that pressure favors dissociation of oligomers[14,19,20] but confirms the recent results obtained by Gebhardt et al.[29] These authors showed that met-myoglobin in the low-pressure regime and in a narrow acidic pH range tends to aggregate. Below a critical pressure, the process is still a reversible association and monomers in equilibrium with small oligomers (formed by less than 10 monomers) occur. Therefore, despite the poor quality of data, we can conclude that the intermediate state is different from the fully unfolded state and can be better regarded as a destabilized state of (partially unfolded) met-myoglobin that is prone to aggregation.

Acknowledgment. We thank M. Kriechbaum (Institute of Biophysics and X-ray Structure Research, Austrian Academy of Sciences, Graz, Austria) and M. Steinhart (Institute of Macromolecular Chemistry, Academy of Sciences of the Czech Republic, Prague, Czech Republic) for their incisive help in setting up the pressure control system on the beamline. P. M. thanks the Italian MIUR for financial support.

References and Notes

(1) Creighton, T. *Proteins*; W.H. Freeman & Co.: New York, 1993.
(2) Kim, P.; Baldwin, R. *Annu. Rev. Biochem.* **1990**, *59*, 631.
(3) Buck, M.; Radford, S.; Dobson, C. *J. Mol. Biol.* **1994**, *237*, 247.
(4) Cinelli, S.; Spinozzi, F.; Itri, R.; Carsughi, F.; Onori, G.; Mariani, P. *Biophys. J.* **2001**, *81*, 3522.
(5) Mariani, P.; Carsughi, F.; Spinozzi, F.; Romanzetti, S.; Meier, G.; Casadio, R.; Bergamini, C. M. *Biophys. J.* **2000**, *78*, 3240.
(6) Tanford, C. *Adv. Protein Chem.* **1968**, *23*, 121.
(7) Weber, G.; Drickamer, H. Q. *Rev. Biophys.* **1983**, *16*, 89.
(8) Brandts, J. In *Structure and Stability of Biological Macromolecules*; Timasheff, S. N., Fasman, G. D., Eds.; Marcel Dekker: New York, 1969; Vol. 2, p 213.
(9) Nash, D.; Jonas, J. *Biochem. Biophys. Res. Commun.* **1997**, *238*, 289.
(10) Nash, D.; Jonas, J. *Biochemistry* **1997**, *36*, 14375.
(11) Kunugi, S.; Yamamoto, H.; Makino, M.; Tada, T.; Uehara-Kunugi, Y. *Bull. Chem. Soc. Jpn.* **1999**, *72*, 2803.
(12) Privalov, P. L.; Griko, Y. V.; Venyaminov, S. Y. *J. Mol. Biol.* **1986**, *190*, 487.
(13) Zipp, A.; Kauzmann, W. *Biochemistry* **1973**, *12*, 4217.
(14) Smeller, L. *Biochim. Biophys. Acta* **2002**, *1595*, 11.
(15) Smeller, L.; Rubens, P.; Heremans, K. *Biochemistry* **1999**, *38*, 3816.
(16) Laurents D. V.; Baldwin, R. L. *Biophys. J.* **1998**, *75*, 428.
(17) Silow, M.; Oliveberg, M. *Proc. Natl. Acad. Sci. U.S.A.* **1997**, *94*, 6084.
(18) Eliezer, D.; Chiba, K.; Tsuruta, H.; Doniach, S.; Hodgson, K.; Kihara, H. *Biophys. J.* **1993**, *65*, 912.
(19) Silva, J.; Weber, G. *Annu. Rev. Phys. Chem.* **1993**, *44*, 89.
(20) Wber, R. *Protein Interactions*; Chapman and Hall: New York, 1992.
(21) Hawley, S. A. *Biochemstry* **1971**, *10*, 2436.
(22) Privalov, P. *J. Mol. Biol.* **1996**, *258*, 707.
(23) Clery, C.; Renault, F.; Masson, P. *FEBS Lett.* **1995**, *370*, 212.
(24) Ruan, K.; Lange, R.; Bec, N.; Balny, C. *Biochem. Biophys. Res. Commun.* **1997**, *239*, 150.
(25) Vidugiris, G. J. A.; Royer, C. A. *Biophys. J.* **1998**, *75*, 463.
(26) Kobashigawa, Y.; Sakurai, M.; Nitta, K. *Protein Sci.* **1999**, *8*, 2765.
(27) Zhou, J.; Zhu, L.; Balny, C. *Eur. J. Biochem.* **2000**, *267*, 1247.
(28) Takano, T. *Methods and Applications in Crystallographic Computing*; Oxford University Press, Oxford, U.K., 1984.
(29) Gebhardt, R.; Doster, W.; Friedrich, J.; Petry, W.; Schulte, A. *Pressure-Induced Critical Association of Myoglobin*, *Advances in High Pressure Science and Biotechnology*; Springer: 2003; Vol. II.
(30) Trewella, J. *Curr. Opin. Struct. Biol.* **1997**, *7*, 702.
(31) Kataoka, M.; Hagihara, Y.; Mihara, K.; Goto, Y. *J. Mol. Biol.* **1993**, *229*, 591.
(32) Kataoka, M.; Nishii, I.; Fujisawa, I.; Ueki, T.; Tokunaga, T.; Goto, Y. *J. Mol. Biol.* **1995**, *249*, 215.
(33) Pollack, L.; Tate, M. W.; Darnton, N. C.; Knight, J. B.; Gruner, S. M.; Eaton, W. A.; Austin, R. H. *Proc. Natl. Acad. Sci. U.S.A.* **1999**, *96*, 10115.
(34) Pèrez, J.; Vachette, P.; Russo, D.; Desmadril, M.; Durand, D. *J. Mol. Biol.* **2001**, *308*, 721
(35) Koch, M.; Vachette, P.; Svergun, D. *Q. Rev. Biophys.* **2003**, *36*, 147.
(36) Spinozzi, F.; Gazzillo, D.; Giacometti, A.; Mariani, P.; Carsughi, F. *Biophys. J.* **2002**, *82*, 2165.
(37) Spinozzi, F.; Maccioni, E.; Teixeira, C. V.; Amenitsch, H.; Favilla, R.; Goldoni, M.; Muro, P. D.; Salvato, B.; Mariani, P.; Beltramini, M. *Biophys. J.* **2003**, *85*, 2661.
(38) Floriano, W. B.; Nascimento, M. A. C.; Domont, G. B.; Goddard, W. A. *Protein Sci.* **1998**, *7*, 2301.
(39) Svergun, D.; Barberato, C.; Koch, M. H. J. *J. Appl. Cryst.* **1995**, *28*, 768.
(40) Svergun, D.; Richard, S.; Koch, M. H. J.; Sayers, Z.; Kuprin, S.; Zaccai, G. *Proc. Natl. Acad. Sci. U.S.A.* **1998**, *95*, 2267.
(41) Spinozzi, F.; Carsughi, F.; Mariani, P.; Teixeira, C. V.; Amaral, L. Q. *J. Appl. Crystallogr.* **2000**, *33*, 556.
(42) Pedersen, J. S.; Schurtenberger, P. *Macromolecules* **1996**, *29*, 7602.
(43) Guinier, A.; Fournet, G. *Small angle scattering of X-ray*; Wiley: New York, 1955.
(44) Feigin, L. A.; Svergun, D. I. *Structure analysis by small-angle X-ray, neutron scattering*; Plenum Press: New York, 1987).
(45) Steinhart, M.; Kriechbaum, M.; Pressl, K.; Amenitsch, H.; Laggner, P.; Bernstorff, S. *Rev. Sci. Instrum.* **1999**, *70*, 1540.
(46) Gekko, K.; Hasegawa, Y. *J. Phys. Chem.* **1989**, *93*, 426.
(47) Press, W. H.; Teukolsky, S. A.; Vetterling, W. T.; Flannery, B. P. *Numerical Recipies. The Art of Scientific Computing*; Cambridge University Press: Cambridge, U.K., 1994.
(48) More, P. *J. Appl. Crystallogr.* **1980**, *13*, 168.
(49) Chalikian, T. V.; Breslauer, K. J. *Curr. Opin. Struct. Biol.* **1998**, *8*, 657.
(50) Pace, C. N.; Laurents, D. V. *Biochemistry* **1989**, *28*, 2520.
(51) Desai, G.; Panick, G.; Zein, M.; Winter, R.; Royer, C. A. *J. Mol. Biol.* **1999**, *288*, 461.
(52) Kunugi, S.; Tanaka, N. *Biochim. Biophys. Acta* **2002**, *1595*, 329.
(53) Freire, E. In *Methods in Molecular Biology: Protein Structure, Stability, and Folding*; Murphy, K. P., Ed.; Humana Press Inc.: Totowa, New Jersey, 2001; Vol. 168, pp 37−68.
(54) Heremans, K.; Smeller, L. *Biochim. Biophys. Acta* **1998**, *1386*, 353.
(55) Paci, E.; Velikson, B. *Biopolymers* **1997**, *41*, 785.